BRS1 mediates plant redox regulation and cold responses

Dongzhi Zhang
State key laboratory of crop stress biology for arid areas, College of agronomy, Northwest A&F University

Yuqian Zhao
State key laboratory of crop stress biology for arid areas, College of agronomy, Northwest A&F university

Junzhe Wang
State key laboratory of crop stress biology for arid areas, College of agronomy, Northwest A&F university

Peng Zhao
State key laboratory of crop stress biology for arid areas, College of agronomy, Northwest A&F University

Shengbao Xu (xushb@nwsuaf.edu.cn)
State key laboratory of crop stress biology for arid areas, College of agronomy, Northwest A&F university
https://orcid.org/0000-0003-2167-5341

Research article

Keywords: Serine carboxypeptidase, Cold stress response, Redox, Arabidopsis

Posted Date: January 5th, 2021

DOI: https://doi.org/10.21203/rs.3.rs-59649/v2

Abstract

Background: Brassinosteroid-insensitive 1 suppressor 1 (BRS1), is a serine carboxypeptidase that mediates brassinosteroid signaling and participates in multiple developmental processes in Arabidopsis. However, little is known about the precise role of BRS1 in this context.

Results: In this study, we analyzed transcriptional and proteomic profiles of Arabidopsis seedlings overexpressing *BRS1* and found that this gene is involved in both cold stress responses and redox regulation. Further proteomic evidence shows that BRS1 regulates cell redox by indirectly interacting with cytosolic NADP+-dependent isocitrate dehydrogenase (cICDH). We identified two novel splice products of *BRS1,* which might play important roles in development and stress responses in plants.

Conclusions: This study highlights the role of BRS1 in plant redox regulation and stress responses, which extends our understanding of extracellular serine carboxypeptidases.

Background

Serine carboxypeptidases (SCP) are a class of eukaryotic proteolytic enzymes, belonging to the *α/β* hydrolase family. These enzymes contain a highly conserved catalytic amino acid triad, Ser-Asp-His [1]. In Arabidopsis, 54 SCP-like genes have been identified and categorized into three classes [2, 3]. However, the functions of majority of these genes have not been described.

BRS1 belongs to class II of the Arabidopsis SCP family [1]. Its overexpression can suppress the phenotype of brassinosteroid (BR) receptor mutant, *bri1-5*, indicating BRS1 play an important role in BR signaling [4, 5]. BRS1 has five close homologs, of which three can suppress *bri1-5* developmental defects [6]. In contrast, no significant phenotypes have been identified in single or double mutants of either BRS1 or its homologs [5-7]. This suggests that BRS1 and its homologs are functionally redundant in Arabidopsis, making difficulties to clarify the precise roles of BRS1.

Increasing evidence has revealed that SCP and SCP-like (SCPL) proteins play crucial roles in the regulation of stress responses, including regulating wound healing [8], programmed cell death and response to pathogen infections [9, 10]. BRS1 contains a signal peptide and localizes to the extracellular space [4, 5]. Since the extracellular space is central in regulating plant stress responses [11-13], it is likely BRS1 might mediate some of these signaling pathways.

Environmental stress leads to the accumulation of reactive oxygen species (ROS) in plant cells and results in oxidative stress [14-16]. Therefore, to adapt to environmental stress, it is vital to control redox homeostasis to maintain normal cellular metabolism, and/or trigger programmed cell death [17, 18].

In this study, transcriptomic and proteomic analyses demonstrate a role for BRS1 in cold stress responses. Our results indicate BRS1 participates in redox regulation via interaction with cICDH, shedding new light on the function of SCPs in plant stress responses.

Results

Seedling developmental phenotypes of BRS1

The mutant *brs1-1D* has an enhancer in *BRS1* promoter [4, 5], resulting in about 15 times increase in *BRS1* transcription compared to that in wild type WS2 (Fig. 1a), showing larger rosette leaves (Fig. 1b) and a longer hypocotyl (Fig. 1c-f). In contrast, BRS1 knockdown mutant, *brs1-1* [4-7], showing a significant transcriptional decrease in *BRS1* (Fig. 1a), but no significant phenotype was observed.

Analysis of the transcriptomes of BRS1 seedlings

We performed RNA sequencing on the BRS1 seedlings (Fig. 1b). A total of 21,873 transcripts were identified, of which 180 differentially expressed genes (DEGs, fold change ≥2.0, FDR-adjusted *p*-value <0.05, FPKM ≥ 1) were identified in the *brs1-1D* seedlings when compared to wild type. This included increased expression of 114 genes and decreased expression of 66 genes (Supplementary Table S1). In contrast, no significantly transcriptional changed gene was identified in *brs1-1* seedlings, except *BRS1* itself (Supplementary Table S1). This is consistent with the finding that no visible morphological difference was shown in *brs1-1* plants (Fig. 1b-f).

However, this was an unusual result because other genes seems not be affected in the *brs1-1* plants. Therefore, the RNA sequencing data was used to investigate the transcriptional details of mutated *BRS1*. The transcription of *BRS1* in *brs1-1* was decreased significantly due to the insertion of a thymidine at position 786 in the first intron (Fig. 2a and b), which resulted in a mis-splicing event (Fig. 2c). In contrast, the transcriptional level of *BRS1* increased by around 20 times in the *brs1-1D* mutant (Fig. 2a), which is consistent with the presence of four copies of CaMV 35S enhancers inserted in the promoter region of *BRS1* (Fig. 2b) [5].

Interestingly, the transcriptional level of the first exon in *brs1-1* maintained a similar level to that of the wild type (Fig. 2c), indicating there is not a feedback loop to enhance *BRS1* transcription. No increased transcription was observed either on the homologs of *BRS1* in *brs1-1* (Supplementary Figure S1).

Notably, two novel splice variants were detected in *brs1-1D*, which retained multiple introns (Fig. 2c). The new splice products (4 and 5) made up a lower proportion of the total *BRS1* transcripts in *brs1-1D*, while the level still equal to the total transcripts of *BRS1* in wild type (Fig. 2c), indicating these novel splice products may have important functions.

BRS1 mediates multiple plant stress responses

Gene Ontology (GO) enrichment analysis of DEGs from *brs1-1D* showed a significant enrichment in genes associated with responding to salicylic acid and jasmonic acid (Fig. 3a). We also found enrichment in genes associated with both biotic (innate immune responses, bacterium, fungus, and chitin) and abiotic (water deprivation, cold and hyperosmotic salinity) stresses (Fig. 3a). In agreement

with these findings, genes associated with redox regulation and cell death were also enriched. These results strongly suggest that BRS1 participates in the responses to environmental stresses.

To support the role of BRS1 in stress response, qRT-PCR was performed on the genes involved in redox regulation, ethylene synthesis and cold response (Fig. 3b). This analysis verified the transcriptional changes in different genotypes (Table S1), suggesting that our RNA-seq data provided a reliable transcriptional difference.

Notably, three core genes of cold signaling, the C-repeat binding factors *CBF1*, *CBF2* and *CBF3* [19], all displayed significantly increased transcription in *brs1-1D*. We therefore checked the cold signaling and response with different cold regimes. The result showed all these cold transcriptional factors increased two times transcriptional level in *brs1-1D* (Fig. 4a) after a freeze treatment (4 °C for 3 h), compared to those in wild type plant. Consistently, cold signaling downstream genes *RD29A* [20], *COR413* [21], *KIN2* [22] showed similar increase trend, while the genes in redox and ethylene signaling keeps the same transcriptional level after freeze treatment (Fig. 4B), indicating the BRS1 has a role in enhancing the cold sensitivity. Further, the phenotypes of seedling after a severe cold shock (-6 °C for 2 h) were investigated, we found the root elongation in *brs1-1D* is significantly longer than that in wild type after 36 hours cold shock (Fig. 4c), suggesting that over-expressed *BRS1* contributes to a higher cold tolerance.

BRS1 regulates redox-related proteins

To further understand the function of BRS1, proteomic analysis was performed on WS2, *brs1-1* and *brs1-1D* seedlings using two-dimensional difference gel electrophoresis (2D-DIGE) (Fig. 5a). Nineteen proteins were assigned as differentially expressed proteins (t-test, p value <0.01), and 14 proteins were identified, of which 5 proteins were involved in redox regulation (Table 1), supporting that BRS1 is involved in redox regulation.

The 2D-DIGE revealed two spots (6 and 7), which were most changed compared to wild type, showing a decrease and increase in *brs1-1D*, respectively (Fig. 5b). These spots corresponded to the same protein, the cytosolic NADP+-dependent isocitrate dehydrogenase (cICDH, at1g65930) (Table 1), a critical redox regulator [23]. Together, these data suggest that BRS1 is involved in redox regulation.

BRS1 participates in redox regulation by interacting with cICDH

To confirm that BRS1 regulates cICDH, the enzyme activity of cICDH was measured in BRS1 mutants. We found that cICDH activity was significantly increased in *brs1-1D* compared to wild type plants (Fig. 6a), whilst no change was observed in *brs1-1* plants. These findings are consistent with our earlier results that only overexpression of BRS1 can alter transcription. Altogether this suggests that BRS1 regulates the activity of cICDH.

To investigate how the secretory protein BRS1 could regulate cICDH, which is localized to the cytosol [24, 25], the cellular localization of BRS1 was evaluated. We observed the expression of BRS1 at the membrane and cell wall (Fig. 6b), consistent with localization to the extracellular space [4, 5], indicating

there is not a physical contact between BRS1 and cICDH. Consistently, yeast two-hybrid and pull-down assays found no direct interaction between cICDH and BRS1 (Supplementary Table S2), indicating that BRS1 regulates cICDH indirectly.

Discussion

BRS1, as a member of SCP, its role is relative clear in SCP family, and its function in plant growth and development has been demonstrated previously [5-7]. In this study, the transcriptome suggested its important role in stress response, highlighting BRS1 as the apoplastic protease, share the important function in biotic and abiotic stress defense [13, 26].

Our results suggest that the BRS1-related stress response is involved in SA and JA signaling (Fig. 3a). These are key hormones required for the induction of plant defenses in response to pathogens and insects [27, 28]. Similarly, an apoplastic SCPL in rice, OsBISCPL1, also induces a stress response via SA and JA signaling [9], indicating SCPLs may use a common mechanism to regulate stress responses.

The trigger effector production by apoplastic proteases used be the key mechanism to induce plant stress response [13]. Our results showed that both cold sensitivity and cold tolerance are significantly enhanced with BRS1 overexpression, then the underlying mechanism need be further investigated to clarify the precise role of BRS1 in cold perception and/or cold signaling.

Consistent with this notion, we found BRS1 regulates redox homeostasis, and therefore plays a critical role in controlling apoplastic ROS [13]. ROS regulation is vital to induce widespread stress responses, and essential for SA and JA signaling in response to various stressors [29, 30]. The ICDHs catalyze the production of NADPH, which is important for redox regulated cell metabolism and promoting redox signaling in response to oxidative stress [31, 32]. cICDH is responsible for more than 90% of total ICDH activity [31, 33]. Therefore, this enzyme plays a crucial role in maintaining redox homeostasis in the cell, and consequently, defense responses [23]. Exactly how BRS1 participates in this pathway still needs further investigation.

The knockdown mutant of *BRS1* does not have any significant phenotypes [5-7]; consistently, we found no transcriptional changes in the mutant *brs1-1* (Supplementary Table S1). However, this finding suggests that there are no pathways dependent on BRS1. In contrast, we observed many phenotypes and identified numerous alterations in gene expression upon overexpression of *BRS1* [7]. The existence of multiple redundant homologs in Arabidopsis may explain this result [5-7]. However, in this study the concurrence of the novel splice variants, phenotypes and activity of cICDH in *brs1-1D* (Fig. 2c), implying a splicing-based functional variation of BRS1, which may play a special role in those highly redundant gene family to overcome their redundancy nature in changing environments.

Conclusions

In this study, transcriptomic and proteomic analyses revealed that BRS1 plays a role in regulating plant responses to cold stress and redox response. We found that BRS1 likely participates in redox regulation in cells through indirect interaction with cICDH. Altogether, our work sheds new light on the roles of SCPs in biotic and abiotic stress responses.

Methods

Plant Materials and Growth Condition

The plant materials used in this study are as follows: Wild-type Wassilewskija (WS2) and mutants of *BRS1* (*brs1-1* and *brs1-1D*). The *brs1-1D* is generated by crossing WS2 with an activation-tagging line *bri1-5 brs1-1D* (CS6127) from the laboratory of Jia Li (Lanzhou University, Lanzhou, China) [4, 5, 7]. The mutant *brs1-1* also came from the laboratory of Jia Li, which was originally obtained from the Wisconsin Arabidopsis knockout pool. This mutant identified insertion a thymidine at 786 bp in first intron through our RNA sequencing and has been used in previous research [7]. T-DNA insertion mutant *icdh-2* (SALK_056247) was ordered from the Salk Institute collection of Arabidopsis Biological Resource Center (ABRC) and verified by genotyping as previously described [23]. Theses seeds were grown in growth chamber at 22 °C under 16 h light/8 h dark conditions (light intensity 100 μmol·m^{-2}·s^{-1}, humidity 60%) for two weeks after germination to perform phenotypic observation. Seedlings of the three materials were cultured on half-strength Murashige and Skoog (1/2 MS) agar medium (supplemented with 1% (w/v) sucrose and 0.8% (w/v) agar, PH5.6-5.8) in the same chamber and culture conditions, and total protein and RNA were extracted seven days after germination.

RNA Extraction and Gene Expression Profiling

Seven-day-old WS2, *brs1-1*, and *brs1-1D* seedlings grown vertically on a 1/2 MS plate were frozen in liquid nitrogen, and triplicate of each material were collected. Total RNA was extracted from whole seedlings using a Tiangen RNAprep pure Plant Kit, and its quality was evaluated with Thermo Scientific NanoDrop2000. The RNA sequencing was completed by Biomarker company (Beijing, China).

Analysis of Transcriptome Data

Raw transcriptome sequencing data was cleaned using Trimmomatic (v 0.36) under default parameters. The clean reads were aligned to the TAIR 10 reference genome using HISAT2 (v 2.1.0) and the expression of genes were profiled using StringTie (v1.3.3) [34, 35]. The reads in the AT4G30610 (*BRS1*) gene region using StringTie for transcript assembly and reads coverage using “genomeCoverageBed” statistics in BEDtools (v 2.29.0).

Identification of Differentially Expressed Genes (DEGs) and GO enrichment analysis

Identification all of differential genes in *brs1-1* and *brs1-1D* compared to control WS2, respectively. The corrected read count data of genes were imported into the R package DESeq2 (v1.26.0) to identify DEGs

with the standard of a fold change ≥ 2.0, a false discovery rate (FDR)-adjusted *p*-value < 0.05, and expression (FPKM ≥ 1) in at least one sample for each comparison [36].

The GO descriptions were obtained by AnnotationHub (“AH75734”), and used the R package clusterProfiler (v3.14.0) with the “enrichGO” function for GO enrichment analysis. The statistical significance of the enrichment of GO was examined using the hypergeometric distribution test, followed by multiple-test correction using the Benjamini–Hochberg method. GO terms with q -value < 0.01 for further enrichment analysis.

Protein Preparation for Fluorescent Two Dimension Difference Gel Electrophoresis (2D-DIGE) Analysis

Seven-day-old seedlings (1 g) were harvested and ground into fine powder in liquid nitrogen and further mixed with 4 mL ice-cold extract buffer (20 mM Tris-HCl, PH 8.0, 1 mM EDTA, 20 mM NaCl, 5 mM MgCl2, 10 mM DTT, 2 mM phenylmethanesulfonyl fluoride, 1 μg/mL leupeptin, 10 μg/mL aprotinin, 1 μg/mL chymostatin and 1% phosphorylase inhibitor mixture). The supernatant was collected by centrifugation at 18,000g for 20 min at 4 °C, and the pellet was resuspended in 3 mL extract buffer for repeat extraction. The combined supernatant was supplemented with chilled acetone to 80% (V/V) (4 times volume acetone of the supernatant) and incubated at -20 °C overnight to precipitate proteins. Proteins were pelleted by dissolved in 100 μL lysis buffer (7 M urea, 2 M thiourea, 4% w/v CHAPS, 20 mM Tris-HCl, pH 8.5), and the debris was removed by centrifugation at 18,000g for 20 min. Finally, the pH of protein samples was adjusted to 8.5 with HCl and NaOH, and the concentration of proteins via Bio-Rad Bradford method using BSA as a standard [37]. The final proteins underwent 2D-DIGE immediately or were stored in aliquots at -80 °C. For each sample, at least quadruplicate protein preparations were performed.

2D-DIGE and Image Analysis

According to the manufacturer's instructions (GE Healthcare), the equivalent amounts of *brs1-1* and *brs1-1D* proteins were labeled with Cy3 and Cy5 minimum fluorescent dyes (400 pmol dye/50 μg protein), respectively. The internal standard WS2 protein was labeled with CY2 and mixed with two different labeled proteins in equal amounts. Adjust the mixed-labeled protein to a total volume of 450 μL with rehydration buffer (8 M urea, 13 mM DTT, 4% w / v CHAPS, 0.5% Pharmalyte pH 3-10), and then load on an IPG test strip holder containing an IPG test strip with 24 cm pH 4-7 linear gradient (GE Healthcare). Experimental methods of isoelectric focusing and SDS-PAGE as previously described [38]. To minimize systemic and inherent biological differences, it is recommended to combine four independent protein preparations for each sample [39].

Fluorescent images of gels were scanned by Typhoon 9400 scanner (GE Healthcare) and the images were analyzed using DeCyder 6.5 software in accordance with the DeCyder User Manual (GE Healthcare) [38]. Approximately 2000 spots were detected in each image, and then spots that showed significant differential expression were determined by ANOVA and Student's t-test ($p < 0.05$). 19 spots with significant differential expression were selected for mass spectrometric identification.

Protein Identification

Coomassie brilliant blue staining was performed on the scanned 2-D-DIGE gel, and then differential protein spots were found by position comparison, but it was difficult to detect proteins with low background expression. Therefore, a 2-DE gel prepared with 1 mg of internal standard protein was used for staining to show spots that could not be determined from the 2D-DIGE gel.

After 19 differential protein spots were excised from 2-D-DIGE gel, each spot was destained in destaining buffer (25 mM ammonium bicarbonate, 50% v/v acetonitrile). Destained spots were dehydrated by acetonitrile and spun-dry, and digested with sequencing grade modified trypsin (Roche) at 37℃ for 16 h. The matrix-assisted laser-desorption ionization (MALDI) mass spectra were produced on an Ultroflex II MALDI time-of-flight/time-of-flight mass spectrometer (MALDI-TOF/TOF MS) (Bruker Daltonics, Germany) with use of FlexAnalysis 2.4 software. After tryptic peptide masses were transferred to a BioTools 3.0 interface (Bruker Daltonics), peptide mass fingerprintings (PMFs) were searched against the NCBInr protein database (http://www.ncbi.nlm.nih.gov/; NCBInr 20071214; 5,742,110 sequences) by use of Mascot software2.2.03(http://www.matrixscience.com; Matrix Science, London,U.K.).

Enzyme activities

Seedlings (0.1 g) at 7 days after germination were ground into fine powder in liquid nitrogen and mixed with the extract buffer (1 mL 0.1 M NaH2PO4 (pH 8.0), 5 mM MgCl2, 14 mM 2-mercaptoethanol). Vortex the homogenate, centrifuge at 12,000 g for 5 minutes to remove insoluble materials, and measure ICDH activity by spectrophotometry [23, 25]. Determination of protein concentration as previously described Bio-Rad Bradford method using BSA as a standard [37].

Confocal imaging

For protein localization of BRS1, the corresponding seedlings root tips from transgenic Col-0 plants expressing 35S-BRS1-GFP were stained in 0.1mg/ml propidium iodide for 8 min. Seedlings were photographed using a confocal fluorescence microscope (Leica, TCS SP8).

Abbreviations

SCP: Serine carboxypeptidase; BRS1: Brassinosteroid-insensitive 1 suppressor 1; ROS: Reactive oxygen species; DEGs: Differentially expressed genes; FPKM: Fragments per kilobase of exon per million fragments mapped; SA: Salicylic acid; JA: Jasmonic acid; cICDH: Cytosolic NADP+-dependent isocitrate dehydrogenase

Declarations

Ethics approval and consent to participate

Not applicable.

Consent for publication

Not applicable.

Availability of data and materials

All data generated or analyzed in this study are included in this article and the supplemental files. The raw data of RNA sequencing were submitted to the NCBI database with the bioproject ID: PRJNA657702.

Competing interests

The authors declare that they have no competing interests.

Funding

This work was funded by the National Key Research and Development Program of China (2016YFD0101602) and the National Natural Science Foundation of China (31370318). This Funding was not involved in the design of the study and collection, analysis, and interpretation of data and in writing the manuscript.

Author Contributions

SX conceived and designed the research and contributed to writing and revising the manuscript. DZ and YZ performed experimental work and data analysis, DZ and JW wrote and revised the manuscript. PZ performed bioinformatics analysis. All authors have read and approved the manuscript.

Acknowledgements

We thank Jia Li (Lanzhou University, Lanzhou, China) for kindly providing the mutants of *BRS1*.

References

1. Fraser CM, Rider LW, Chapple C. An expression and bioinformatics analysis of the Arabidopsis serine carboxypeptidase-like gene family. Plant Physiol 2005; 138(2):1136-48.
2. Tripathi LP, Sowdhamini R. Cross genome comparisons of serine proteases in Arabidopsis and rice. BMC Genomics 2006; 7:200.
3. Zhu D, Chu W, Wang Y, Yan H, Chen Z, Xiang Y. Genome-wide identification, classification and expression analysis of the serine carboxypeptidase-like protein family in poplar. Physiol Plant 2018; 162(3):333-52.
4. Zhou A, Li J. Arabidopsis BRS1 is a secreted and active serine carboxypeptidase. J Biol Chem 2005; 280(42):35554-61.
5. Li J, Lease KA, Tax FE, Walker JC. BRS1, a serine carboxypeptidase, regulates BRI1 signaling in *Arabidopsis thaliana*. Proc Natl Acad Sci U S A 2001; 98(10):5916-21.

6. Wen J, Li J, Walker J. Overexpression of a serine carboxypeptidase increases carpel number and seed production in *Arabidopsis thaliana*. Food and Energy Security 2012; 1(1):61-9.
7. Deng Q, Wang X, Zhang D, Wang X, Feng C, Xu S. BRS1 Function in Facilitating Lateral Root Emergence in Arabidopsis. Int J Mol Sci 2017; 18(7):1549.
8. Moura DS, Bergey DR, Ryan CA. Characterization and localization of a wound-inducible type I serine-carboxypeptidase from leaves of tomato plants (*Lycopersicon esculentum* Mill.). Planta 2001; 212(2):222-30.
9. Liu H, Wang X, Zhang H, Yang Y, Ge X, Song F. A rice serine carboxypeptidase-like gene *OsBISCPL1* is involved in regulation of defense responses against biotic and oxidative stress. Gene 2008; 420(1):57-65.
10. Domínguez F, González MC, Cejudo FJ. A germination-related gene encoding a serine carboxypeptidase is expressed during the differentiation of the vascular tissue in wheat grains and seedlings. Planta 2002; 215(5):727-34.
11. Zhu JK. Abiotic Stress Signaling and Responses in Plants. Cell 2016; 167(2):313-24.
12. Zhou JM, Zhang Y. Plant Immunity: danger perception and signaling. Cell 2020; 181(5):978-89.
13. Wang Y, Wang Y, Wang Y. Apoplastic Proteases - Powerful Weapons Against Pathogen Infection in Plants. Plant Communications 2020:100085.
14. Apel K, Hirt H. Reactive oxygen species: metabolism, oxidative stress, and signal transduction. Annu Rev Plant Biol 2004; 55:373-99.
15. Waszczak C, Carmody M, Kangasjärvi J. Reactive Oxygen Species in Plant Signaling. Annu Rev Plant Biol 2018; 69:209-36.
16. Sies H, Berndt C, Jones DP. Oxidative Stress. Annu Rev Biochem 2017; 86:715-48.
17. Suzuki N, Koussevitzky S, Mittler R, Miller G. ROS and redox signalling in the response of plants to abiotic stress. Plant Cell Environ 2012; 35(2):259-70.
18. Qi J, Wang J, Gong Z, Zhou JM. Apoplastic ROS signaling in plant immunity. Curr Opin Plant Biol 2017; 38:92-100.
19. Chinnusamy V, Zhu J, Zhu JK. Cold stress regulation of gene expression in plants. Trends Plant Sci 2007; 12(10):444-51.
20. Msanne J, Lin J, Stone JM, Awada T. Characterization of abiotic stress-responsive *Arabidopsis thaliana* RD29A and RD29B genes and evaluation of transgenes. Planta 2011; 234(1):97-107.
21. Breton G, Danyluk J, Charron JB, Sarhan F. Expression profiling and bioinformatic analyses of a novel stress-regulated multispanning transmembrane protein family from cereals and Arabidopsis. Plant Physiol 2003; 132(1):64-74.
22. Kurkela S, Borg-Franck M. Structure and expression of kin2, one of two cold- and ABA-induced genes of *Arabidopsis thaliana*. Plant Mol Biol 1992; 19(4):689-92.
23. Mhamdi A, Mauve C, Gouia H, Saindrenan P, Hodges M, Noctor G. Cytosolic NADP-dependent isocitrate dehydrogenase contributes to redox homeostasis and the regulation of pathogen

responses in Arabidopsis leaves. Plant Cell Environ 2010; 33(7):1112-23.

24. Gálvez S, Hodges M, Decottignies P, Bismuth E, Lancien M, Sangwan RS, Dubois F, LeMaréchal P, Crétin C, Gadal P. Identification of a tobacco cDNA encoding a cytosolic NADP-isocitrate dehydrogenase. Plant Mol Biol 1996; 30(2):307-20.
25. Galvez S, Bismuth E, Sarda C, Gadal P. Purification and Characterization of Chloroplastic NADP-Isocitrate Dehydrogenase from Mixotrophic Tobacco Cells (Comparison with the Cytosolic Isoenzyme). Plant Physiol 1994; 105(2):593-600.
26. Stael S, Van Breusegem F, Gevaert K, Nowack MK. Plant proteases and programmed cell death. J Exp Bot 2019; 70(7):1991-95.
27. Browse J. Jasmonate passes muster: a receptor and targets for the defense hormone. Annu Rev Plant Biol 2009; 60:183-205.
28. Zhang Y, Li X. Salicylic acid: biosynthesis, perception, and contributions to plant immunity. Curr Opin Plant Biol 2019; 50:29-36.
29. Noctor G, Reichheld JP, Foyer CH. ROS-related redox regulation and signaling in plants. Semin Cell Dev Biol 2018; 80:3-12.
30. Pieterse CM, Van der Does D, Zamioudis C, Leon-Reyes A, Van Wees SC. Hormonal modulation of plant immunity. Annu Rev Cell Dev Biol 2012; 28:489-521.
31. Marino D, González EM, Frendo P, Puppo A, Arrese-Igor C. NADPH recycling systems in oxidative stressed pea nodules: a key role for the NADP+ -dependent isocitrate dehydrogenase. Planta 2007; 225(2):413-21.
32. Hodges M, Flesch V, G S, Bismuth E. Higher plant NADP+-dependent isocitrate dehydrogenases, ammonium assimilation and NADPH production. Plant Physiology & Biochemistry 2003; 41(6-7):577-85.
33. Hodges M. Enzyme redundancy and the importance of 2-oxoglutarate in plant ammonium assimilation. J Exp Bot 2002; 53(370):905-16.
34. Kim D, Langmead B, Salzberg SL. HISAT: a fast spliced aligner with low memory requirements. Nat Methods 2015; 12(4):357-60.
35. Pertea M, Pertea GM, Antonescu CM, Chang TC, Mendell JT, Salzberg SL. StringTie enables improved reconstruction of a transcriptome from RNA-seq reads. Nat Biotechnol 2015; 33(3):290-5.
36. Love MI, Huber W, Anders S. Moderated estimation of fold change and dispersion for RNA-seq data with DESeq2. Genome Biol 2014; 15(12):550.
37. Bradford MM. A rapid and sensitive method for the quantitation of microgram quantities of protein utilizing the principle of protein-dye binding. Anal Biochem 1976; 72:248-54.
38. Xu SB, Yu HT, Yan LF, Wang T. Integrated proteomic and cytological study of rice endosperms at the storage phase. J Proteome Res 2010; 9(10):4906-18.
39. Barceló-Batllori S, Kalko SG, Esteban Y, Moreno S, Carmona MC, Gomis R. Integration of DIGE and bioinformatics analyses reveals a role of the antiobesity agent tungstate in redox and energy

homeostasis pathways in brown adipose tissue. Mol Cell Proteomics 2008; 7(2):378-93.

Table

Table 1. List of differentially expressed proteins identified by mass spectrometry (MS)

No.	Chromosome locus	Matched protein	Biological process	Expression Fold
1	AT3G08590	2,3-Biphosphoglycerate-independent phosphoglycerate mutase 2	Carbohydrate metabolism	1.18
2	AT3G57610	Adenylosuccinate synthetase	AMP biosynthesis	0.87
3	AT3G54050	Chloroplastic fructose 1,6-bisphosphate phosphatase	Fructose metabolism	0.88
4	AT2G39730	Rubisco activase	Light activation of rubisco	1.21
5	AT5G15650	UDP-arabinose mutase	Arabinose metabolism	0.68
6*	**AT1G65930**	**Cytosolic NADP+-dependent isocitrate dehydrogenase**	**Redox**	**0.22**
7*	**AT1G65930**	**Cytosolic NADP+-dependent isocitrate dehydrogenase**	**Redox**	**3.12**
8	**AT1G03475**	**Coproporphyrinogen III oxidase**	**Redox**	**1.15**
9	AT5G09530	Proline-rich protein 10	Seed germination	1.24
10	AT1G66200	Cytosolic glutamate synthetase	Glutamine biosynthesis	1.79
11	ATCG00490	Ribulose-bisphosphate carboxylase	Carbon fixation of photosynthesis	0.79
12	AT3G44310	Nitrilase 1	Nitrogen compound metabolism	1.37
13	**AT1G75280**	**Isoflavone reductase**	**Redox**	**1.26**
14	**AT1G78380**	**Glutathione s-transferase tau 19**	**Redox**	**1.16**
15	AT1G20340	DNA-damage resistance protein 112	Response to UV	0.67

The differentially expressed proteins were assigned according to the $p < 0.01$ (Student's *t*-test, two tails). Proteins in bold refer proteins are involved in redox. 'Expression Fold' is calculated as the ratio of the expression level in *brs1-1D* to the control WS2. Triplicate biological repeats were performed with independent protein preparations.

Figures

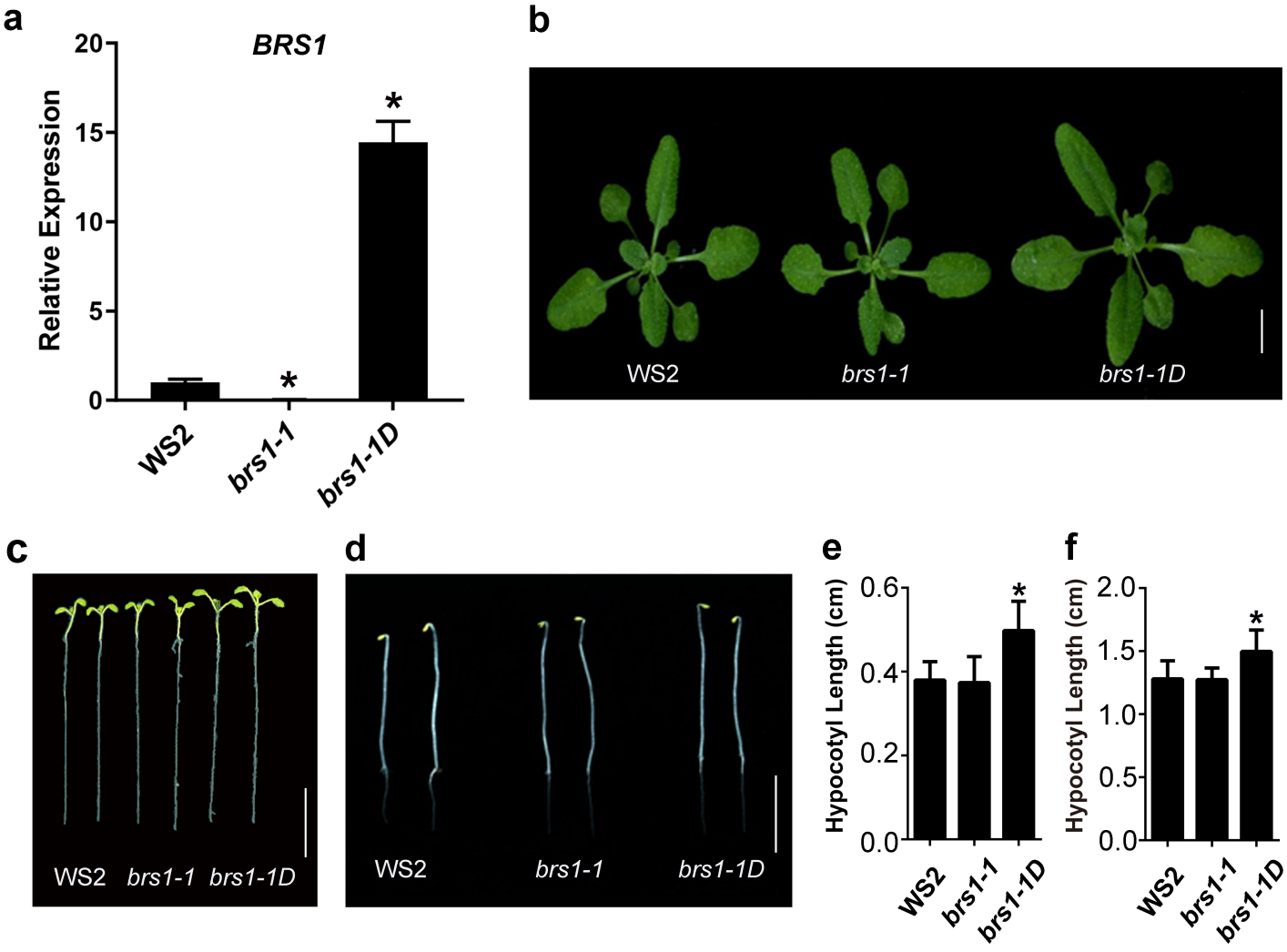

Figure 1

The seedling phenotypes in wild type and BRS1 mutants a. The relative transcriptional level of BRS1 in wild type WS2, brs1-1 and brs1-1D. All results are shown as mean ± standard deviation (SD) from three biological replicates with qRT-PCR. The asterisks indicate a statistically significant difference (Student's t-test, *p < 0.05). b. The seedling phenotypes of WS2, brs1-1 and brs1-1D at 14 days after germination (DAG). Scale bar = 1 cm. c. The phenotypes of WS2, brs1-1 and brs1-1D grown on 1/2 MS medium under long-day conditions. Photos captured 7 DAG. Scale bar = 1 cm. d. The hypocotyl phenotypes of WS2, brs1-1 and brs1-1D seedlings grown on 1/2 MS medium in the dark. Photos captured 5 DAG. Scale bar = 1 cm. e. Comparison of hypocotyl lengths in (c). Means ± SD are shown from three independent experiments, n≥ 20 in each experiment. The asterisks indicate a statistically significant difference (Student's t-test, *p < 0.05). f. Comparison of the hypocotyl lengths in (d). Means ± SD are shown from three independent experiments, n ≥ 20 in each experiment. The asterisks indicate a statistically significant difference (Student's t-test, *p < 0.05).

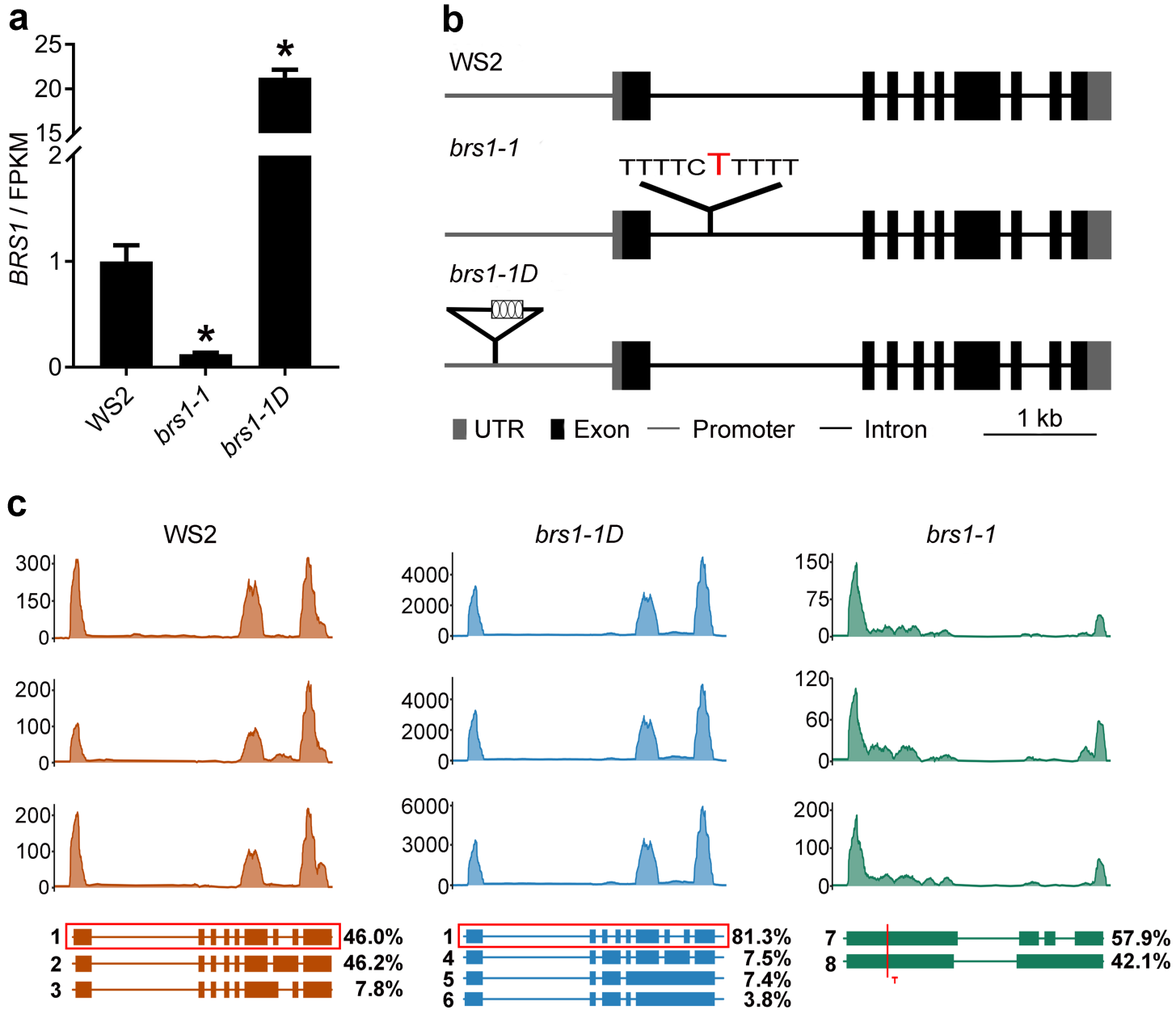

Figure 2

Differences in gene sequences and BRS1 transcription in wild type and BRS1 mutants a. Transcription levels (FPKM value) of BRS1 in WS2, brs1-1 and brs1-1D as measured by RNA-seq. All results are shown as mean ± SD from three biological replicates. The asterisks indicate a statistically significant difference (Student's t-test, *p < 0.05). b. The difference of BRS1 sequences in WS2, brs1-1 and brs1-1D. A single thymidine base (red) is inserted in the first intron of brs1-1, and the 4 X 35S enhancer (four ellipses in black box) is inserted in the promoter of BRS1 in brs1-1D. c. The transcription of BRS1 in RNA-seq data. The counts of different reads of BRS1 and their distribution in genes are shown above. The types of different BRS1 transcripts present in the different samples are shown below. The percentage shows the

ratio of individual transcript to total transcripts. The red box highlights the normal transcript of BRS1 in TAIR10. Three biological replicates were analyzed.

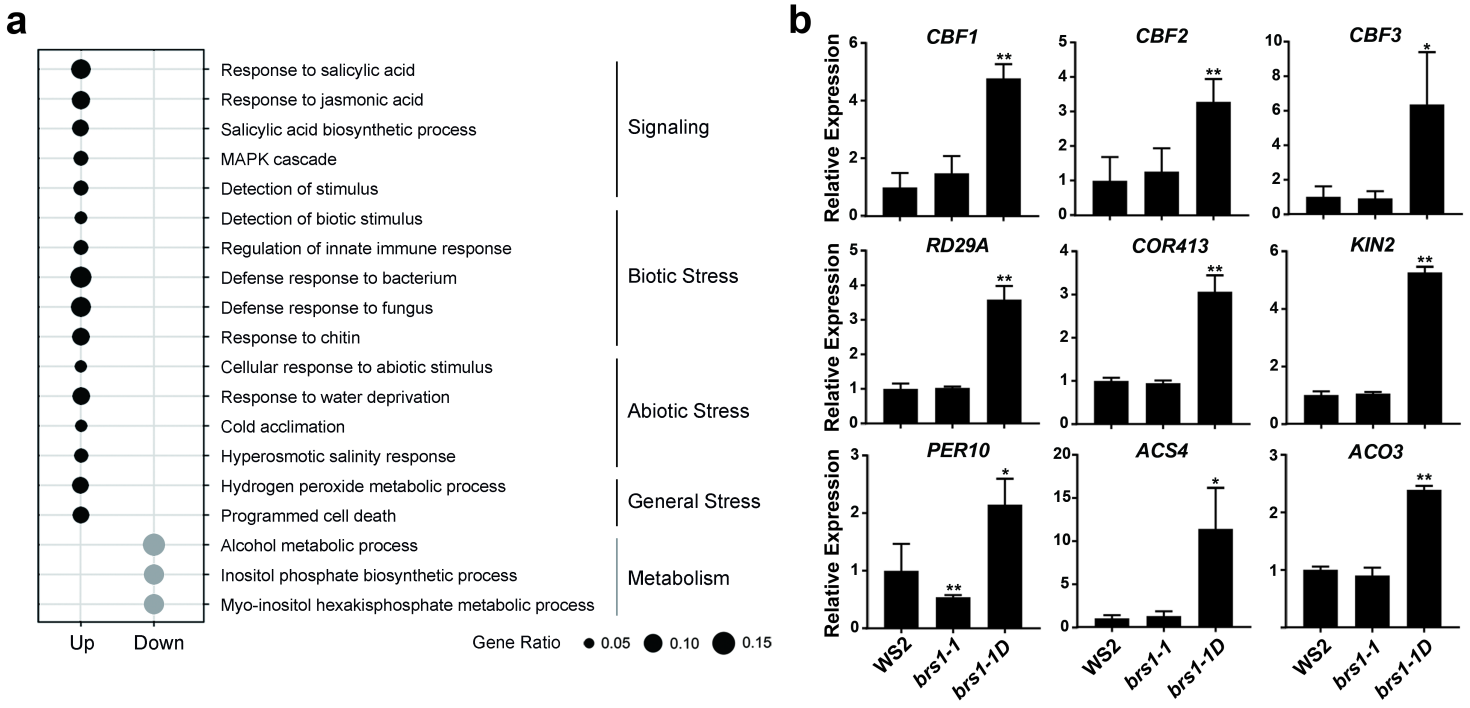

Figure 3

Enrichment analysis of the DEGs between brs1-1D and wild type a. Analysis of GO terms associated with DEGs between brs1-1D and WS2 seedlings (q-value < 0.01). The black dot represents DEGs that are up-regulated in brs1-1D compared to WS2; the grey dot represents DEGs that are down-regulated. Terms found enriched in the up-regulated DEGs are divided into four categories (black vertical lines). The term enriched in the down-regulated DEGs is indicated with the grey vertical line. Gene ratio indicates the ratio of DEGs clustered into different terms, divided by the total number of DEGs. b. The qRT-PCR analysis on cold related genes (CBF1, CBF2, CBF3, RD29A, COR413, KIN2), redox related gene (PER10) and ethylene synthesis related genes (ACS4, ACO3). These genes were significant up-regulated in brs1-1D compared to WS2, consistent with RNA sequencing results (Table S1). All results are presented as mean ± SD from from three biological replicates at least. The asterisks indicate a statistically significant difference (Student's t-test, **p < 0.01, *p < 0.05).

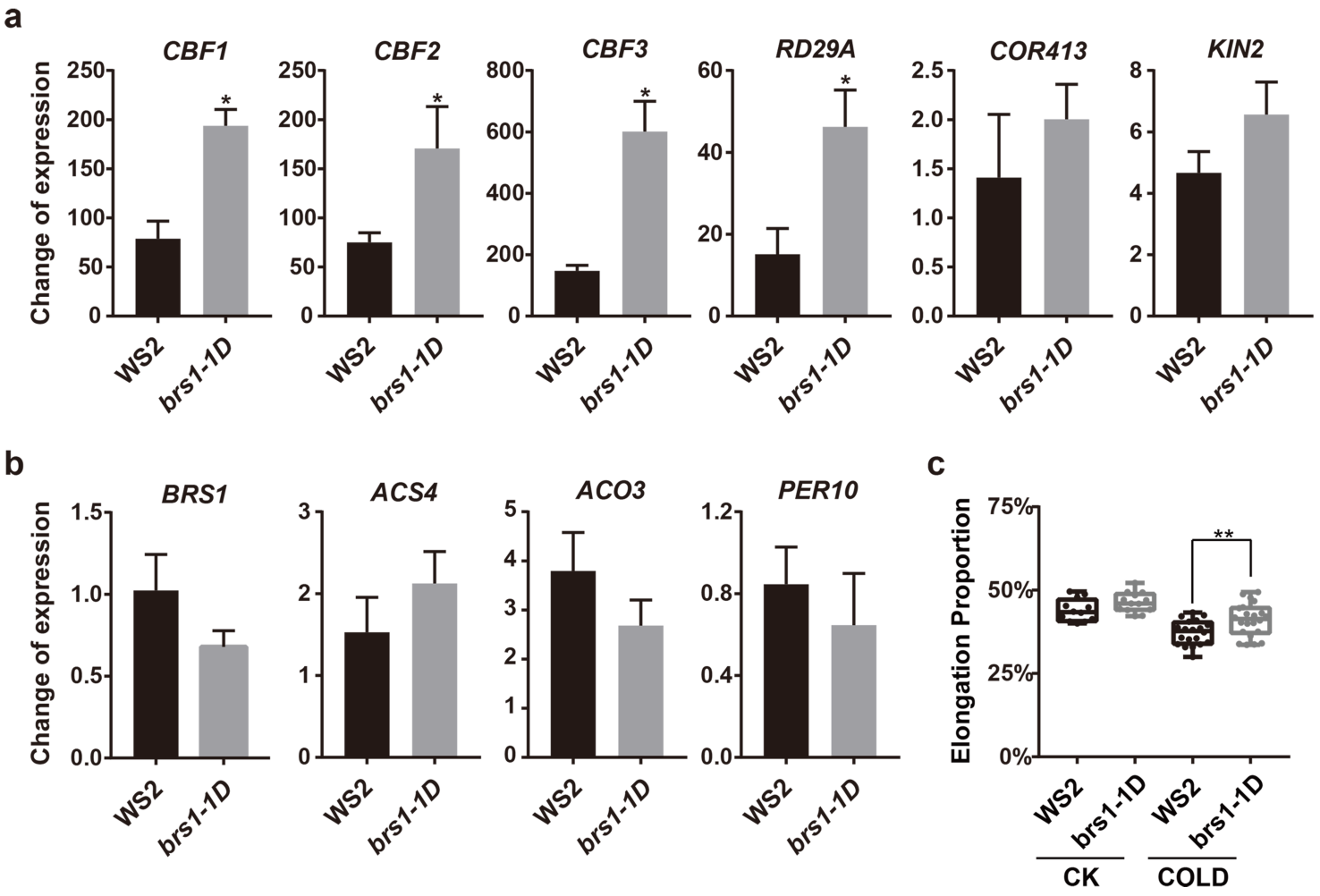

Figure 4

The brs1-1D shows a higher cold sensitivity and cold tolerance. a. The qRT-PCR showed the different cold response on cold signaling genes, and b. The qRT-PCR showed changes of BRS1, ethylene synthesis related genes (ACS4 and ACO3) and redox related gene PER10 between brs1-1D and wild type after freeze treatment (4 °C for 3 hours). Each column represents the changed fold after freeze treatment compared to untreated control. All results are shown as mean ± SD from three biological replicates at least. The asterisks indicate a statistically significant difference (Student's t -test, *p < 0.05). c. The root elongation proportion in WS2 and brs1-1D after a severe cold treatment (-6 °C for 2 hours). 7 DAG seedlings were shifted to -6 °C for 2 hours and then returned to normal conditions (22 °C) for 36 hours. The root elongation proportion refers to the root elongation after cold treatment compared to the length of the root before the treatment. Data is from three biological replicates. The same results were repeated in two times. The asterisks indicate a statistically significant difference (Student's t-test, ** p < 0.01).

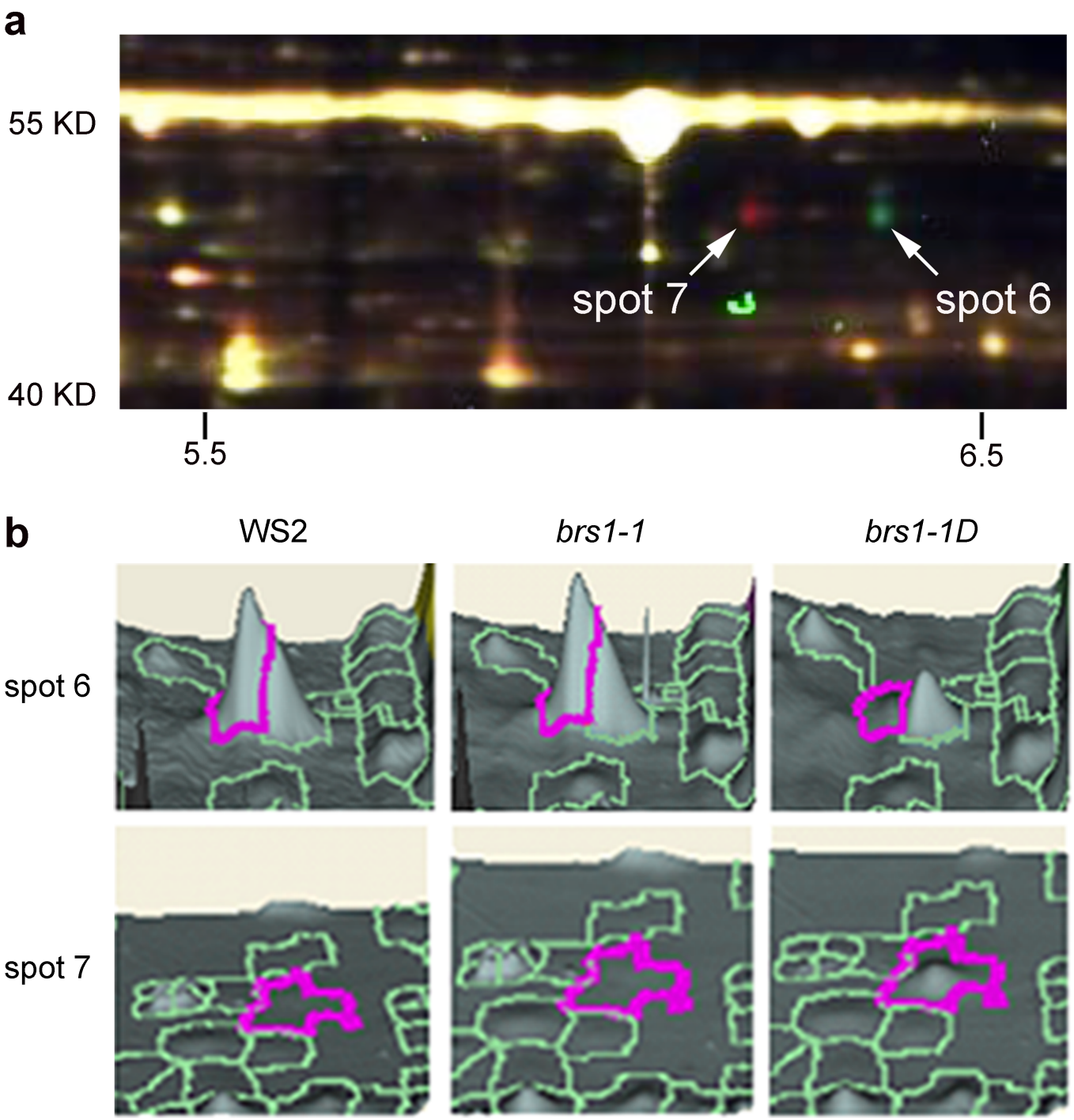

Figure 5

Identification of two isoforms of cICDH and comparison of protein expression levels a. Representative 2D-DIGE image. Samples from WS2, brs1-1 and brs1-1D were labeled with Cy2 (blue), Cy3 (green), and Cy5 (red), respectively. The x- and y-axis represent the isoelectric point and molecular weight of the protein, respectively. White arrows indicate differential protein spots. b. Expression levels of two

differential protein spots in WS2, brs1-1 and brs1-1D. The height of the pink circled area represents the level of protein expression.

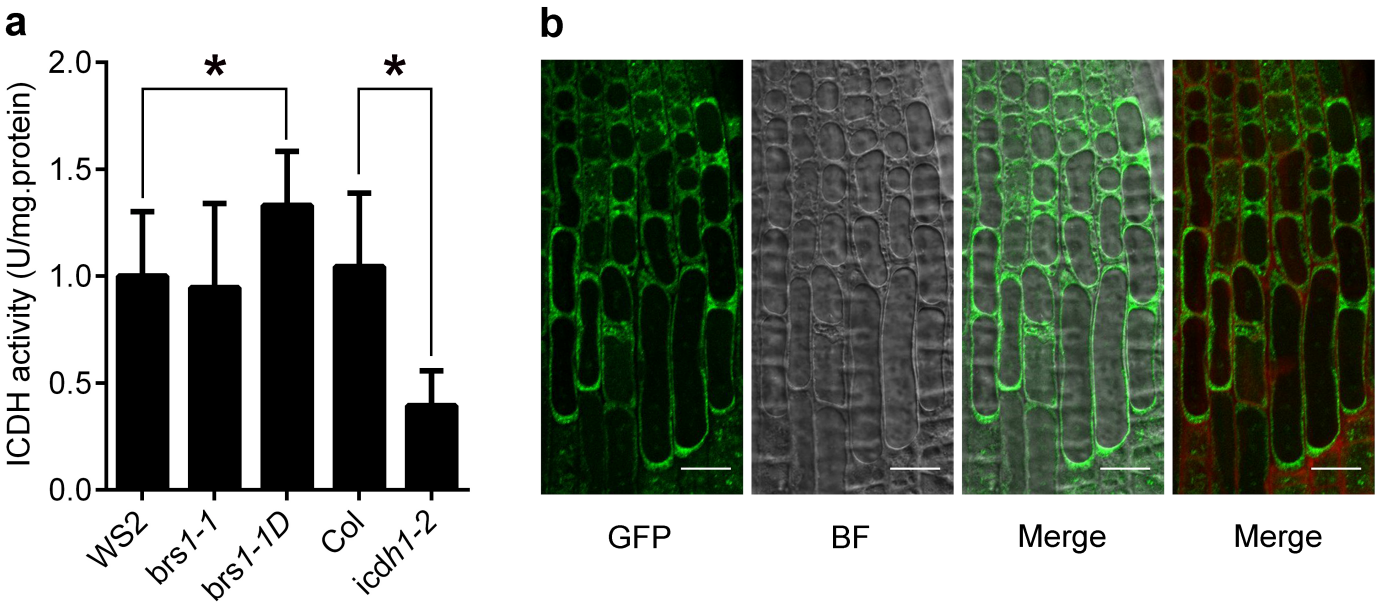

Figure 6

The enzyme activity of cICDH depends on BRS1 a. Total extractable ICDH activity from wild type (WS2 and Col-0) seedlings and a range of mutant lines: brs1-1D, brs1-1 and icdh-2. Means and SD of eight independent extracts are shown. Asterisks indicate a statistically significant difference based on Student's t-test (*$p < 0.05$). b. Subcellular localization of BRS1. Root tips from transgenic Col-0 plants expressing 35S-BRS1-GFP were used to visualize the subcellular localization of BRS1-GFP by confocal microscopy. The green fluorescence indicates the BRS1-GFP and the red fluorescence indicates propidium iodide staining.

Supplementary Files

This is a list of supplementary files associated with this preprint. Click to download.

- TableS1.xlsx
- FigureS1.tif
- TableS2.xlsx